Atmospheric Environment 301 (2023) 119696

Contents lists available at ScienceDirect

Atmospheric Environment

journal homepage: www.elsevier.com/locate/atmosenv

Source apportionment of potentially toxic PM_{10} near a vast metallic ore mine and health risk assessment for residents exposed

Carlos Boente [a,b], Adrián Zafra-Pérez [a,*], Juan Carlos Fernández-Caliani [a,c], Ana Sánchez de la Campa [a,c], Daniel Sánchez-Rodas [a,d], Jesús D. de la Rosa [a,c]

[a] CIQSO-Center for Research in Sustainable Chemistry, Associate Unit CSIC-University of Huelva "Atmospheric Pollution", Campus El Carmen s/n, 21071, Huelva, Spain
[b] Department of Mining, Mechanic, Energetic and Construction Engineering, ETSI, University of Huelva, Huelva, 21071, Spain
[c] Department of Earth Sciences, Faculty of Experimental Sciences, University of Huelva, Huelva, 21071, Spain
[d] Department of Chemistry, Faculty of Experimental Sciences, University of Huelva, Huelva, 21071, Spain

HIGHLIGHTS

- Metallic mines are a source of PM_{10} in potentially toxic elements.
- PM_{10} was collected in three villages around the Rio Tinto mine during one year.
- The village closest to the mine presented the highest PM_{10} and PTE concentrations.
- PMF analysis revealed two mining sources presenting high contributions.
- Inhalation exposure to PM_{10} in nearby residents is at a safe level.

GRAPHICAL ABSTRACT

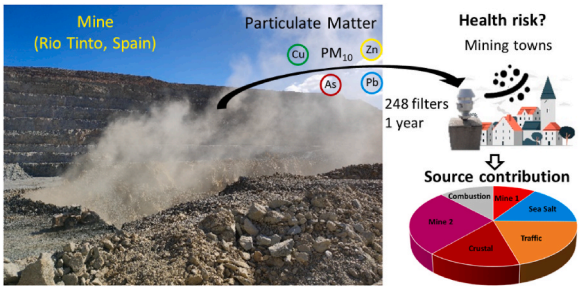

ARTICLE INFO

Keywords:
Source contribution
Health risk assessment
PM_{10}
Mining
Atmospheric pollution

ABSTRACT

Mining is an economic activity that traditionally releases large amounts of particulate matter into the atmosphere because of the procedures required to process the mineral. In particular, polymetallic ores are environmentally harmful as they can enrich potentially toxic elements, which may cause adverse effects to humans and ecosystems due to their toxicity. The aim was to assess the impact on health of this type of mining on nearby populations. Accordingly, it was conducted an extensive PM_{10} sampling campaign during the entirety of 2021 through a total of 248 filters placed in three villages close to the Rio Tinto district (Southwest Spain), which is one of the largest Cu mines in the world. A total of 58 major and trace elements were analysed, along with organic carbon/elemental carbon, cations, and anions. The mean PM_{10} concentrations were high during spring (47 $\mu gPM_{10} \cdot m^{-3}$) and summer (56 $\mu gPM_{10} \cdot m^{-3}$) in the population closest to the mine, wherein values surpassed the annual and daily limit values, but were lower in the other two villages. Moreover, high enrichment of As (annual maximum mean of 6.2 $ng \cdot m^{-3}$), Cu (70 $ng \cdot m^{-3}$), Pb (19 $ng \cdot m^{-3}$), and Zn (50 $ng \cdot m^{-3}$) was observed in all locations. A positive matrix factorization (PMF) was primarily used to assess the origins of this particulate matter, revealing that the impact of the mine reduced considerably over a long distance, with contributions ranging from 36% at the mine's outskirts to 8% further away from it, which coincides with the features of the mine during the abandonment phase (2001–2015). Despite this, the risk assessment revealed that the

* Corresponding author. CIQSO-Center for Research in Sustainable Chemistry, Associate Unit CSIC-University of Huelva "Atmospheric Pollution", Campus El Carmen s/n 21071, Huelva, Spain.
E-mail address: adrian.zafra@dfaie.uhu.es (A. Zafra-Pérez).

https://doi.org/10.1016/j.atmosenv.2023.119696
Received 17 January 2023; Received in revised form 23 February 2023; Accepted 28 February 2023
Available online 5 March 2023

carcinogens were within the permissible exposure limits even in the closest village, indicating a minor concern for the inhabitants from a toxicological perspective.

1. Introduction

Monitoring of potentially toxic elements (PTEs) and their risk assessment in environmental compartments is a topic that has garnered special attention at global, regional, and local scales. The ability of PTEs to persist and bioaccumulate in biota is a threat to ecosystems and human health, and their anomalous concentrations in soils (e.g. Kabata-Pendias, 2010) and waters (Blais et al., 2008) has been widely described. Regarding atmospheric pollution, the risk of PTEs is particularly relevant as constituents of inhalable atmospheric particulate matter (PM_{10}), which can easily be suspended in air and travel long distances, thereby affecting many people (Ramírez et al., 2020). The common risks of prolonged exposure to non-toxic PM include respiratory ailments (Moreno et al., 2019; Can-Terzi et al., 2021), cardiovascular mortality (Brook et al., 2010), and adverse effects on newborns (Peled, 2011). Additionally, the toxic features of PTEs are bound to PM_{10}, although the contribution of PTEs to the total mass of PM is less than 1% (Massimi et al., 2022). Moreover, PTEs are among the main determinants of biological responses when an organism is exposed to PM_{10} (Van Den Heuvel et al., 2016), and they may pose a carcinogenic risk (IARC, 2014) and boost the occurrence of cardiorespiratory disorders (Nie et al., 2018; Cakmak et al., 2014; Wild et al., 2009). Thus, understanding PTEs and their sources in PM_{10} are important to preserve human health and ecosystems.

The presence of PTEs in the atmosphere is mainly attributed to industrial activities (mineral extraction, ore processing and smelting, or fossil fuel combustion), traffic emissions, and natural sources, such as windblown dust and volcanic activity (Boente et al., 2020; Ermolin et al., 2018; Ruggieri et al., 2012). These complex scenarios with PM_{10}-bound trace elements from multiple pollution sources require mathematical methodologies that can differentiate the contribution of each source to the total atmospheric pollution (Millán-Martínez et al., 2021; Conca et al., 2019; Men et al., 2018; Cabello et al., 2016). Regardless of the source, some researchers have found a strong correlation between high pollutant concentrations and the economic development level of society (Li et al., 2013). Accordingly, the population factor was considered in several studies dealing with human health risk assessment of PTEs in PM in highly populated cities worldwide (Naraki et al., 2021; Men et al., 2020; Caggiano et al., 2019).

However, these are not the only areas requiring further study. For example, regions with open-pit mining are also an interesting target of study as mining activity attracts the population and has traditionally been linked to atmospheric pollution (Stewart, 2020; Csavina et al., 2012). Open-pit mining can produce a large amount of PM during drilling, waste and ore loading, hauling, and pit dumping (Boente et al., 2022; Huertas et al., 2012). Human health risks associated with PTEs derived from mining activities have been extensively reviewed in the literature, especially in metallic mines, where diseases such as cancer are more frequent (da Silva-Rêgo et al., 2022; Patra et al., 2016; Utembe et al., 2015). However, risk assessment and source contribution studies in metalliferous mining regions are scarce (Ulniković and Kurilić, 2020; Tubis et al., 2020).

This study investigates one of the most prolific open-pit metallic mines in Europe, namely, the Rio Tinto mine (southwest Spain). Mineral particles removed by wind from abandoned mine waste have been a persistent source of air pollution in this historic mining district. They comprise a variety of metal-bearing minerals, with the most common being pyrite and its oxidation products, namely, iron oxyhydroxides and jarosite (Fernández-Caliani et al., 2013). The reopening of the open-pit mine in 2015 raised concerns regarding air quality and related health risks from exposure to dust particles generated during mining activities.

The lack of reliable information on the harmful health effects of air pollutants on people living close to mines indicates the need for a quantitative risk assessment of respirable particulate matter. In recent years, several studies have attempted to assess the potential health risks that may result from the inhalation of soil particles in the Rio Tinto mine and other mine sites in the Iberian Pyrite Belt (Gabari and Fernández-Caliani, 2017; Fernández-Caliani et al., 2019; Parviainen et al., 2022). The approach outlined by these authors was based on indirect estimates of exposure using simplified modelling methods for predicting the contaminant concentrations at points of exposure, such as the ASTM-RBCA box model (Connor et al., 2007). However, this simplification can lead to an overestimation of the outdoor air concentration by a factor of 10 (Verginelli et al., 2017). Here, we used direct measurements of PM_{10} concentrations and chemical composition at or as close as possible to the point of exposure. Thus, our point-of-contact approach can significantly refine site-specific health risk assessments by providing a more accurate evaluation of exposure point concentrations.

The purpose of this study was to analyse the PM_{10} source contribution to distinguish natural and anthropogenic emissions from the mine and quantify the site-specific health risks associated with PTE exposure through the inhalation of PM_{10} by people living around the mining area. The results of this assessment can assist mining companies in making informed decisions about the effects of mining on the ambient air quality and health of nearby residents during mining operations.

2. Materials and methods

2.1. Study area

The Rio Tinto mine (Fig. 1) is located in the Spanish sector of the Iberian Pyrite Belt and constitutes one of the largest volcanogenic massive sulphide (VMS) deposits in the world, with more than 500 Mt of VMS resources and approximately 2 Gt of low-grade stockwork mineralisation, including zones of economic interest averaging 0.41% of Cu, which are currently being exploited at the Cerro Colorado open pit (Atalaya Mining, 2022). The VMS orebody mainly comprises pyrite with minor amounts of chalcopyrite, sphalerite, galena, and traces of arsenopyrite and grey copper ores (De Mello et al., 2022).

The mineral wealth of the district garnered strong attraction even before the Roman era. Copper was believed to first be recovered from the ores in the third millennium BC and silver was known to be mined in the late Bronze Age (Salkield, 1987). Modern mining began in the middle of the 19th century with the arrival of the Rio Tinto Company, and the mine extensively extracted copper and pyrite from 1873 to 2001; it was closed thereafter due to profitability issues. Nevertheless, the use of new technologies to reducing costs and the rise in copper prices enabled the reopening of the mine in 2015, and it is currently fully operational (Sánchez de la Campa et al., 2020).

The large size of the mining area, occupying a surface area of approximately 20 km^2, and the low grade of the ore body being mined involves extensive earthmoving. Moreover, this region is characterised by a dry climate and low precipitation with annual mean temperature and humidity of 24 °C and 58% (Müller, 2022), respectively, as well as a mountainous landscape that enhances the presence of strong air currents. The combination of these factors results in the displacement of significant amounts of PM enriched in PTEs, thereby leading to environmental problems (Boente et al., 2022).

The villages of Minas de Riotinto, Nerva, and La Dehesa, with a total population of almost 9000 inhabitants, are located in the surroundings of the mine, at distances of 1.5, 4, and 0.2 km, respectively. For obtaining these distances, we measured the line joining the closest

mining operation to the monitoring station. Therefore, residents are permanently exposed to atmospheric particulate matter derived from mining activities, which occur uninterruptedly during the whole year. According to the company, the pace of work is similar throughout the year, thus being the dust production in the mine constant.

2.2. Sampling of PM_{10} and chemical analyses

This study was conducted at three monitoring stations (Fig. 1), all of which belong to the Air Quality Network of the Rio Tinto mining district. Sampling and chemical analyses were the same for the three stations and were conducted according to the normalised method UNE-EN 12341 (UNE, 2015). Sampling of PM_{10} was conducted using high purity quartz fibre filters (Munktell®), introduced in the inlets of regulatory high-volume air samplers (MCV CAV-A-PM1025:30 m^3h^{-1}), installed between 5 and 15 m height on rooftops or scaffolds to avoid walls or barriers that may cause particles blocking (Fig. SM1). These devices fulfil UNE-EN ISO 9001:2008 standards from our accredited laboratory and are subjected to an annual revision. One 24-h sample was collected every four days from January to December 2021. A total of 248 filters were collected from the three monitoring stations: 86 were gathered in Minas de Riotinto, 78 in Nerva and 84 in La Dehesa. Slight differences in the number of samples were attributed to unforeseen electrical current failures in sporadic days that may occur during long campaigns in equipment exposed to inclement weather, although a sufficiently large database was obtained to extract robust conclusions. The filters were transported to the laboratory and dried in a room at a temperature and relative humidity of 20 ± 1 °C and 50 ± 5%, respectively, 24 h prior to weighing. The mass of PM_{10} retained on the filters was determined using a Sartorius LA130 S–F balance, which has a sensitivity of 0.1 mg.

The methodology used to determine the chemical composition of PM_{10} comprised several techniques that followed the procedures described by Querol et al. (2002). Half a portion of each filter was acid digested (in 2.5 mL of HNO_3:5 mL of HF:2.5 mL of $HClO_4$) for the analysis of major elements using inductively coupled plasma-optical emission spectrometry (ICP-OES; Agilent model 5110) and trace elements through inductively coupled plasma mass spectroscopy (ICP-MS; Agilent model 7900). To control the quality, an analysis of NIST-1663c (using fly ash as the reference standard material) was conducted during the run of both ICP instruments. External calibration was conducted by ICP-OES using elemental standard solutions (0.05, 0.5, 1, 2, 5, 10, and 25 ppm, and a 5% HNO_3 blank sample). External calibration was conducted by ICP-MS using cocktail solutions (0.25, 0.5, 1, 2, 5, and 10 ppb, as well as a 5% HNO_3 blank sample). The limits of detection (LoD) obtained for most elements ranged from 0.01 to 11 ng/m^3 for ICP-MS, and 1.5 ng/m^3 to 1.85 $\mu g/m^3$ for ICP-OES for all the elements studied; these included Al, As, Ba, Be, Bi, Ca, Cd, Cl, Co, Cr, Cs, Cu, Fe, Ga, Ge, K, La, Li, Mg, Mn, Mo, Na, Nb, Ni, P, Pb, Rb, Sb, Se, Sn, Sr, Th, Ti, Tl, U, V, W, Zn, and Zr, as well as rare earth elements (REEs): Sc, Y, La, Ce, Pr, Nd, Sm, Eu, Gd, Tb, Dy, Ho, Er, Tm, Yb, Lu, Hf, and Ta.

A quarter of each filter was leached with Milli-Q grade deionised water to extract water-soluble ions (NH_4^+, Cl^-, SO_4^{2-}, and NO_3^-) for subsequent analysis by ion chromatography (IC; Methrom 883 Basic IC Plus). For these results, the quality control for soluble water ions was determined through a solution cocktail for low- and high-concentration anions (0.05–2.5 and 0.5–50 ppm) and cations (1–10 ppm). The accuracy and detection limit for IC was 10% and 0.4 $\mu g/m^3$. Additionally, for each filter, an area of 1.5 cm^2 was used to analyse organic carbon (OC)

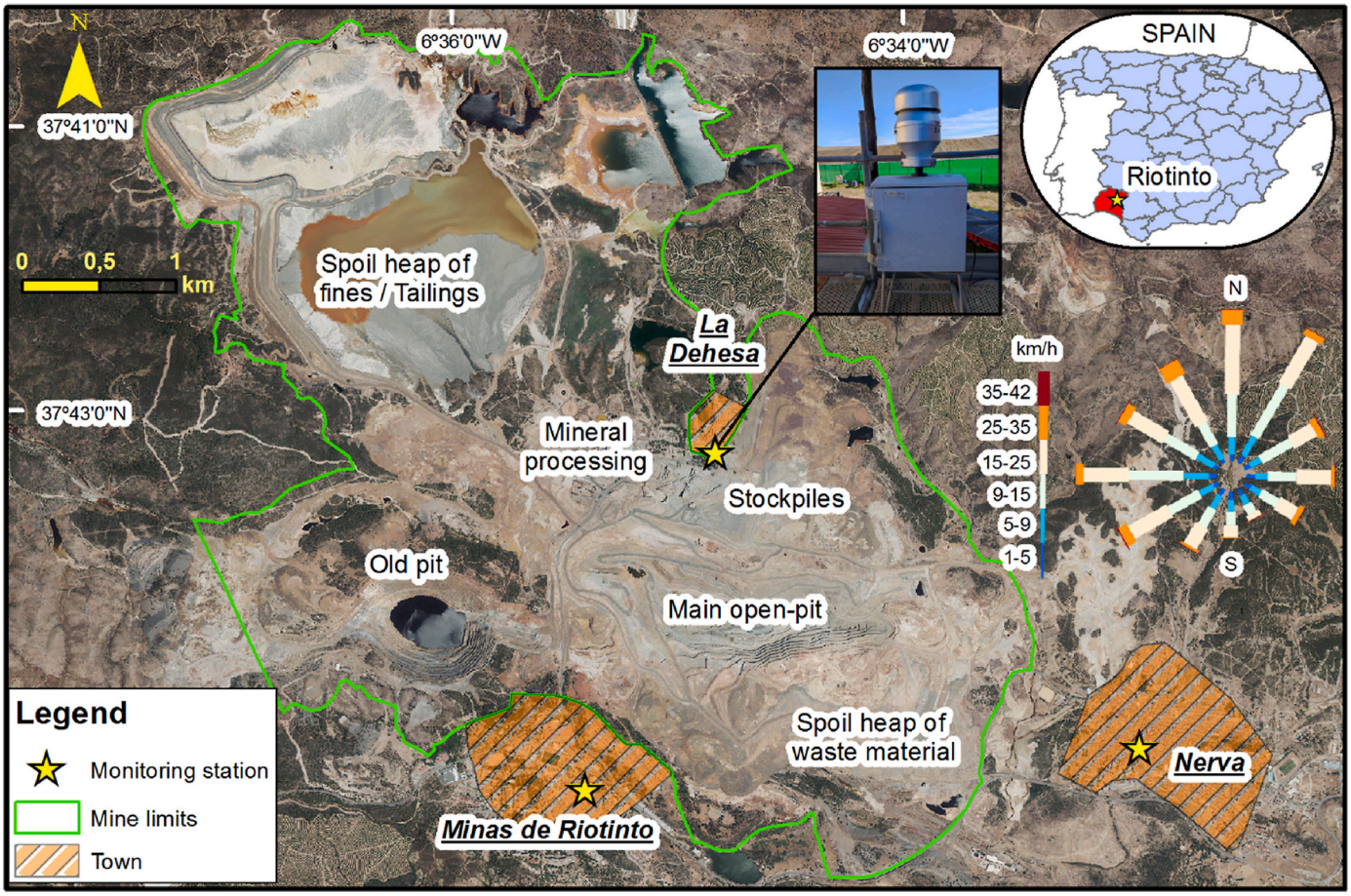

Fig. 1. Main areas of the Rio Tinto mine and the location of the three monitoring stations in the villages, including a photograph of one of the high-volume air samplers and a wind rose for 2021.

and elemental carbon (EC) using a Sunset Laboratory OC-EC analyser according to the EUSAAR-2 protocol (Cavalli et al., 2010). For this methodology, we used a sucrose aqueous solution (4.2 μg/l) to ensure the quality of the measurements and consistent operation of the device.

2.3. Source contribution

A positive matrix factorization (PMF) analysis of the PM_{10} chemical composition was conducted for the three monitoring stations using v5.0 (Norris and Duvall, 2014). For this assessment, air mass origins during the sampling campaign were considered to determine the source contribution. The PMF model is a factor analytical tool developed by Paatero and Tapper (1994) and Paatero (1997) and can be used to calculate the chemical profiles and contributions of different pollutant sources. The basis of PMF is a mathematical algorithm based on Eq. (1):

$$\mathrm{Xij} = \sum_{k-1}^{p} g_{ik} \bullet f_{kj} + e_{ij} \quad (1)$$

The full data can be expressed as an $i \times j$ dimension matrix (x). Here, i is the number of samples; j is the number of chemical elements measured; p corresponds to the number of independent factors; g_{jk} represents the amount of air mass contributed by each factor for each sample; f_{kj} describes the species profiles for each factor; and i_{ej} is the residue for each sample by element.

The PMF comprises a weighted least-squares method wherein every individual estimate of the uncertainty in each data value is required and included in the input matrix. There are different sources of errors contributing to the measurement of uncertainty; however, those associated with the analytical procedure is one of the most important. In this study, uncertainty was calculated in accordance with the methodology developed by Amato et al. (2009), which is in accordance with European and Environmental Protection Agency (EPA) recommendations (Belis et al., 2019; Norris and Duvall, 2014).

Elements were classified using the signal-to-noise (S/N) ratio (Paatero and Hopke, 2003). Elements with S/N > 2 were defined as strong variables and introduced in the PMF analysis, condition which was fulfilled by a total of 26 elements as well as OC/EC, ions and PM_{10} concentration. As the S/N ratio is highly sensitive to sporadic values compared to the level of noise, the percentage of data above the detection limit was used as a complementary criterion.

2.4. Health risk assessment

The inhalation exposure concentration of potentially toxic trace elements in ambient air was calculated by multiplying the trace element concentration in PM_{10} by the exposure multiplier of residential receptors based on Eq. (2) (USEPA, 2009):

$$\mathrm{ECinh} = \frac{\mathrm{Cair} \times \mathrm{ET} \times \mathrm{EF} \times \mathrm{ED}}{\mathrm{AT}} \quad (2)$$

where EC_{inh} is the chronic inhalation exposure concentration (μg/m^3); C_{air} is the average element concentration in PM_{10} at the point of exposure (μg/m^3); ET is the exposure time (24 h/day); EF is the exposure frequency (350 days/year); ED is the exposure duration for adults (15 years) and children (6 years); AT is the time period (days) over which the exposure is averaged for carcinogenic effects (AT = 78 years × 365 days/year × 24 h/day) and non-carcinogenic effects (AT = 15 years or 6 years × 365 days/year × 24 h/day).

The exposure parameters used in Eq. (2) closely match the frequency and duration of exposure (350 days per year for 15 years, which is the operational lifespan of the mine) for people with a life expectancy of 78 years living close to the mining area.

Owing to the uncertainty associated with estimating the true average trace element concentration at the exposure point (C_{air}), the 95% upper confidence limit (UCL) of the arithmetic mean concentration was calculated for this variable using Eq. (3) (USEPA, 1992):

$$\mathrm{UCL} = \mathrm{e}^{\left(\overline{x} + 0.5s^2 + sH/\sqrt{n-1}\right)} \quad (3)$$

where UCL is the upper confidence limit in percentage; e is the base of the natural logarithm; $\overline{x}$ is the mean of the log-transformed data; s is the standard deviation of the log-transformed data; H is the H-statistic value (Gilbert, 1987); and n is the number of samples. The data were log-transformed by considering the natural logarithm of the values because the dataset was found to be consistent with a lognormal distribution (Kolmogorov-Smirnov test, $\alpha = 0.05$).

The cancer risk based on the lifetime average exposure to carcinogenic trace elements through the inhalation of PM_{10} was estimated by multiplying the inhalation exposure concentration by the inhalation unit risk factor (Eq. (4)):

$$\mathrm{CR} = \mathrm{ECinh} \times \mathrm{URF} \times 1000 \quad (4)$$

where CR is the carcinogenic risk; EC_{inh} is the chronic inhalation exposure concentration (mg/m^3) averaged over a 78-year lifetime; and URF is the unit risk factor of inhalation (μg/m^3)$^{-1}$, which is an estimate of the increased cancer risk from inhalation exposure to a concentration of 1 μg/m^3 in air for one lifetime (USEPA, 2009). The URF value was multiplied by 1000 to convert it to units of risk per mg/m^3. This study focuses on human carcinogens categorised by the USEPA, 1986 as Group A (As and Ni) and Group B1 (Be and Cd), whose URF values were obtained from the Integrated Risk Information System (IRIS) database (available at www.epa.gov/iris).

For non-carcinogens, the risk from inhalation of PM_{10}-bound trace elements was based on the hazard quotient, which was calculated by dividing the inhalation reference concentration of trace elements by the inhalation reference concentrations listed in the IRIS and other chemical toxicity databases in accordance with the standard guidelines (USEPA, 1989), as expressed in Eq. (5):

$$\mathrm{HQ} = \frac{\mathrm{ECinh}}{\mathrm{RfC}} \quad (5)$$

where HQ is the hazard quotient (unitless), EC_{inh} is the inhalation exposure concentration (mg/m^3), and RfC is the chronic inhalation reference concentration (mg/m^3). For multiple trace elements (n), the overall inhalation hazard index (HI [Eq. (6)]) was calculated by summing the individual hazard quotients (HQ) for each trace element of concern (i) by assuming additivity of effects:

$$\mathrm{HI} = \sum_{i=1}^{n} \mathrm{HQ}_i \quad (6)$$

If HI exceeds 1.0, there may be a concern for potential non-carcinogenic risk. Otherwise, no adverse health effects are assumed.

3. Results and discussion

3.1. Levels and chemical composition of PM_{10}

European protection laws for the atmospheric environment (Directive, 2008/50/CE) and Spanish legislation in this field (Royal Decree 102/2011, 28th January) demand one of the following two conditions for declaring a potential health risk by PM_{10}: 1) a mean annual limit value (ALV) exceeding 40 μgPM_{10}/m^3; or 2) a daily limit value (DLV) that stipulates that a maximum value of 50 μgPM_{10}/m^3 must not occur more than 35 times in a calendar year. This is also indicative of the 90.4th percentile, whose threshold value is fixed at 50 μgPM_{10}/m^3.

Our results reveal that the mean annual values of PM_{10} were: 27.1 μgPM_{10}/m^3 in Minas de Riotinto ($P_{90.4}$ = 41.4), 29.4 μgPM_{10}/m^3 in Nerva ($P_{90.4}$ = 51.4), and 41.8 μgPM_{10}/m^3 in La Dehesa ($P_{90.4}$ = 78.2). Only the population of La Dehesa exceeds the ALV value of 40 μgPM_{10}/m^3, which exceeds the 90.4th percentile. The other two populations are

well below the threshold limit except for Nerva, whose values exceed the 90.4th percentile. Thus, a potential health risk from PM_{10} exists in La Dehesa, the population closest to the mine, as well as in Nerva but to a minor extent.

Fig. 2 shows the seasonal variations in PM_{10} at the three monitoring stations. The global values are higher during spring and summer owing to the warmer temperature and dry conditions that benefit the resuspension of PM (Vardoulakis and Kassomenos, 2008). Notably, the concentration values of La Dehesa are always significantly higher than those of Minas de Riotinto and Nerva, especially during spring and summer, when the mean surpasses both the ALV and DLV. Apart from its close proximity to the mine, La Dehesa is also within the preferential direction of winds (W-NW) in relation to the location of the spoil heap of fines (see wind rose in Fig. 1) during most of the year, with speeds averaging up to 25 km/h. This undoubtedly contributed to an increase in the PM content.

The standard deviation also presents a high variation, which implies notable differences between the maximum and minimum PM_{10} concentrations and the presence of extreme values. We acknowledge two factors controlling this. On the one hand, the high variability found during February–March (winter) and June–September (summer) is attributable to the high contributions of Saharan dust during these seasons (Viana et al., 2002); however, in October–December (autumn) dust intrusions are less frequent (Rodriguez et al., 2001). On the other hand, precipitation is another factor having influence on aerosol deposition. In this context, accumulated precipitation for different seasons in the study area is shown in Fig. SM2 (Müller, 2022). Here, it can be appreciated that the precipitation during winter (247 mm) is higher than the joint sum of the other three seasons (211 mm) in our study area. It is well known that heavy rains difficult the resuspension of PM_{10} and increase the relative humidity in the atmosphere. Thus, this combination of rainy and dry days typical in winter is another factor implying the presence of extreme values as well as the low mean concentration of PM_{10} during this season.

The presence of high PM_{10} concentrations, especially near mines, is frequently attributed to mechanical disruption operations, such as crushing, grinding, and haulage, which cause the production and resuspension of dust (Sastry et al., 2015) despite the efforts made for dust reduction from mining processes through irrigation with $CaCO_3$--neutralised water (Zafra-Pérez et al., 2023). However, although the concentrations found in this study exceeded thresholds, they were relatively low compared to other mining villages in the world. Most of the studies that can be found in the literature are focused on coal mines. In this context, Pandey et al. (2014) reported concentrations reaching seasonal mean concentrations of 271.9 $\mu g PM_{10}/m^3$ in India. In another coal mine in Colombia, the maximum seasonal mean concentration found in a nearby mining village was 61.14 $\mu g PM_{10}/m^3$ (Huertas et al., 2012), which is consistent with our results. Conversely, studies conducted in metallic mining villages revealed seasonal average concentrations of 187 $\mu g PM_{10}/m^3$ in China (Cheng et al., 2017). The maximum seasonal mean found in this study was 56 $\mu g PM_{10}/m^3$ during summer, which is far from those of previous studies. However, historically, open-pit coal mines tend to generate more PM_{10} than metallic mines because of the mechanical characteristics of coal, which have traditionally led to health problems for people living in the surroundings, especially children (Pless-Mulloli, 2000).

In particular, the study area is relatively close to Africa. This implies that exposure to Saharan dust events provoked extreme PM concentrations. These occur particularly between February and March and June–September (Viana et al., 2002). During the full year of 2021, the number of days with intrusion of Saharan dust from North Africa was 25%, which is within the average for the 1980–2021 period in Mediterranean Europe (Adame et al., 2022). A study of Saharan dust outbreaks during our sampling time was carried out. Computed box-plot diagram (Fig. 3a) for all samples allowed to find two periods presenting extreme values: 3rd week of February and 2nd week of August. According to NOAA's HYSPLIT model (Stein et al., 2015), these peaks are coincident with two North African outbreaks (Fig. 3b), which undoubtedly contribute to the increase of PM_{10} in the Rio Tinto mining district. Thus, except for these two weeks, Saharan intrusions were not significant enough to cause extreme values on our data. Complete datasheet for these two intrusions can be found in the Supplementary Materials section (Figs. SM3 and SM4).

The monitoring stations are located in villages near the mine. Thus, it is essential to study the chemical composition and provenance of PM_{10} reaching the mining villages to discern the real impact of the mine on the environment. Previous studies have highlighted that the most significant PTEs present in massive sulphide mineralisation from the Iberian Pyrite Belt are As, Cu, Pb, and Zn (Sáez et al., 1996; Chopin and Alloway, 2007). The statistical descriptors of PTEs and trace elements for the three monitoring stations during 2021 are listed in Table 1. The results of the major elements are presented in Table SM1. Apart from the enrichment of the aforementioned elements, there were also remarkably high concentrations of Ba, Cr, Mn, Ni, and Ti. The first four elements are enriched in the mining operations developed in the Rio Tinto mine (Boente et al., 2022), whereas Ti is a typical trace element of clayey soils related to iron-bearing minerals, such as pyrite (Mclaughlin, 1954).

Differences can be observed among the monitoring stations, as presented in Table 1. Minas de Riotinto and Nerva present similar annual mean concentrations for almost all elements, with generally low standard deviations that ensure normal distributions. Although the main PTEs of the mineralisation show higher concentrations in Minas de Riotinto compared to those in Nerva, no significant differences were observed between the element concentrations at these two monitoring

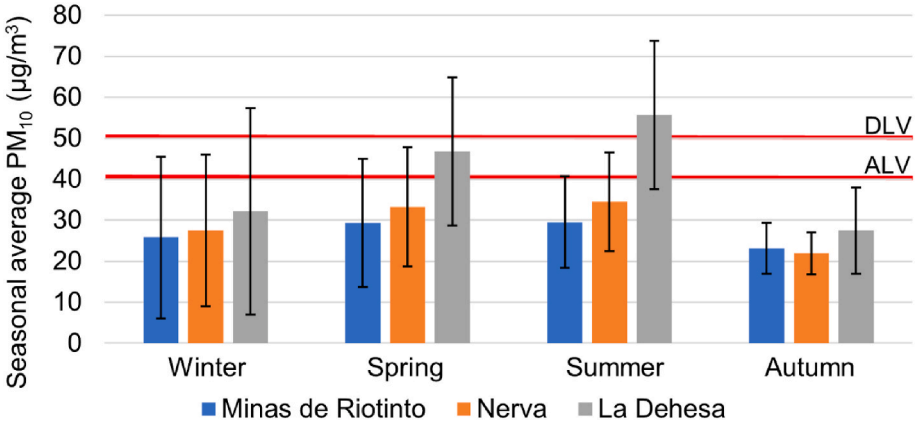

Fig. 2. Seasonal variations of PM_{10} represented as mean and standard deviations in the three monitoring stations during 2021. Red lines correspond to the daily limit value (DLV) and annual limit value (ALV).

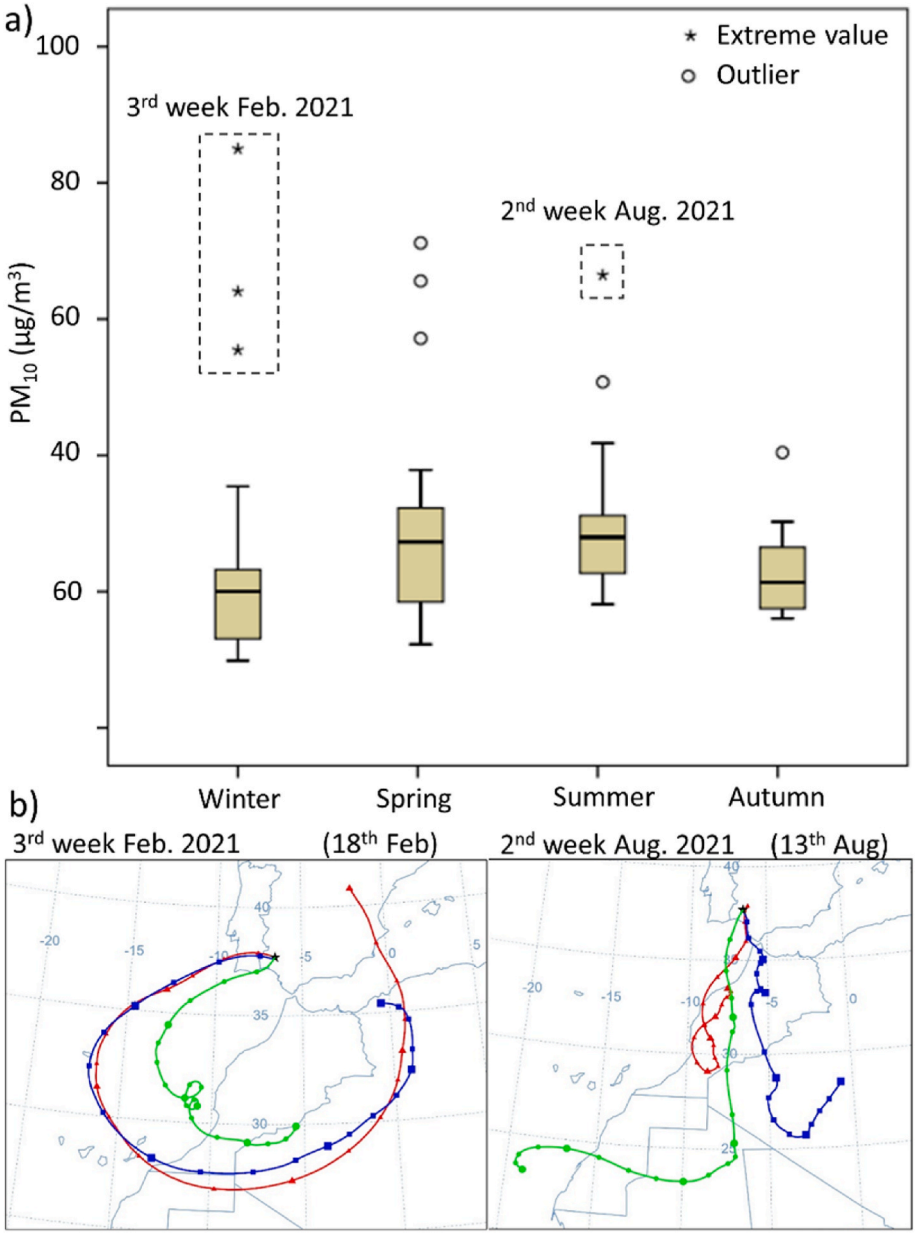

Fig. 3. a) Box plot diagram showing PM_{10} concentrations in Minas de Riotinto, representative for the three monitoring stations. b) Backward trajectories ending at the Rio Tinto mining district for days presenting extreme values.

stations. However, maximum peaks for PTEs of the mineralisation were higher in Minas de Riotinto, especially for Cu (89.6 ng·m^{-3}) and Zn (348 ng·m^{-3}). This is consistent with the fact that this village is closer to the current area of operation than Nerva. However, similar to those of PM_{10}, the concentrations of both PM_{10} and PTEs are very similar and cannot be considered differently.

These differences are noteworthy when considering the concentrations found in the La Dehesa village. The concentrations of all elements are considerably higher than those obtained for the other populations, especially for As (6.2 ng/m^3), Cu (70 ng/m^3), Pb (19 ng/m^3) and Zn (50 ng/m^3). In this context, the coefficient [$Mean_{La\ Dehesa}/Mean_{Minas\ de\ Riotinto}$], which indicates the number of times that the elements exceeded the mean concentration in Minas de Riotinto, reveals the following exceedances for As (4.11, the highest among all the elements studied), Cu (3.41), Pb (3.50), and Zn (1.88). Moreover, the large standard deviations for this station also imply more variability in the data, indicating more differences between the upper and lower concentrations. For the remaining elements, the coefficient is always above 1.0, implying that La Dehesa has the highest potential toxicological risk. Additionally, this village also has the highest levels of PM_{10}.

Fig. 4 depicts the evolution of the four main PTEs in the Rio Tinto mine. The concentrations of all PTEs in La Dehesa were significantly higher than those in Minas de Riotinto and Nerva, and they were especially enriched in As, Cu, and Pb. The values of As, the most hazardous PTE in La Dehesa, are practically at the same level throughout the year, similar to the values of Pb in Nerva and Minas de Riotinto (<10 ng/m^3). In line with the evolution of PM_{10}, the concentrations were also higher during spring and summer than during the cold seasons.

In conclusion, two clear trends were observed. First, Minas de Riotinto and Nerva are the furthest villages from the mine and present similar compositions of PM_{10} and PTEs, with PM_{10} being higher in Nerva and PTEs being more abundant in Minas de Riotinto. These concentrations were similar to those reported by Sánchez de la Campa et al. (2011) during the abandonment phase of the mine. Notably, the practically equal similarities between both villages imply the existence of a geochemical background for PM_{10} affecting the entire mining district,

Table 1
Mean and maximum concentrations, and standard deviation of trace elements analysed in the three monitoring stations during 2021. Units are expressed in ng/m^3.

	Minas de Riotinto			Nerva			La Dehesa		
Element	Mean	Max	Std	Mean	Max	Std	Mean	Max	Std
As	1.5	4.5	0.9	1.5	4.4	0.8	6.2	32	5.6
Ba	11	41	7.7	9.9	36	7.3	26	111	22
Be	<0.1	0.2	<0.1	0.0	0.1	0.0	0.1	0.2	<0.1
Bi	0.2	0.6	0.1	0.1	0.8	0.1	0.5	2.3	0.5
Cd	0.1	0.4	0.1	0.1	0.4	0.1	0.2	1.1	0.2
Co	0.2	1.3	0.2	0.3	1.1	0.2	0.9	3.9	0.9
Cr	1.5	12	2.2	1.6	19	2.4	3.5	108	12
Cs	0.1	0.3	0.0	0.1	0.3	0.1	0.1	0.4	0.1
Cu	21	90	20	11.3	38	8.0	70	275	55
Ga	0.2	1.7	0.3	0.3	1.6	0.3	0.6	2.7	0.5
Ge	0.1	0.6	0.1	0.1	0.6	0.1	0.2	0.7	0.2
Li	0.5	3.4	0.6	0.7	3.2	0.6	1.4	6.1	1.2
Mn	8.4	42	9.0	10	40	9.0	25	125	25
Mo	1.1	29	4.5	1.3	29	5.3	0.3	4.8	0.8
Nb	0.2	1.2	0.2	0.2	1.1	0.2	0.3	1.4	0.2
Ni	2.6	92	10	1.4	12	1.8	3.6	126	15
Pb	5.5	14	3.4	5.2	15	2.9	19	336	38
Rb	1.0	6.1	1.0	1.3	5.8	1.1	1.8	9.9	1.7
Sb	0.7	3.0	0.6	0.5	1.6	0.3	2.7	11	2.4
Se	0.1	0.4	0.1	0.1	0.4	0.1	0.2	0.6	0.1
Sn	0.8	3.4	0.7	0.8	3.0	0.7	1.3	4.7	1.0
Sr	2.8	21	3.8	3.1	20	4.0	3.3	23	4.2
Th	0.1	0.8	0.1	0.1	0.8	0.1	0.3	1.4	0.3
Ti	38	277	54	43	255	51	52	306	63
Tl	<0.1	0.1	<0.1	<0.1	0.1	<0.1	0.1	0.5	0.1
U	0.1	0.3	<0.1	0.1	0.3	0.1	0.1	0.5	0.1
V	1.5	8.0	1.5	1.8	7.6	1.6	2.0	9.9	1.9
W	0.1	0.9	0.1	0.1	0.7	0.1	0.1	0.8	0.1
Zn	26	348	43	20	182	21	50	244	45
Zr	2.9	11	2.9	2.6	8.9	2.9	4.3	18	3.5
ΣREEs	3.0	18	2.9	3.3	17	2.9	5.7	25	4.8

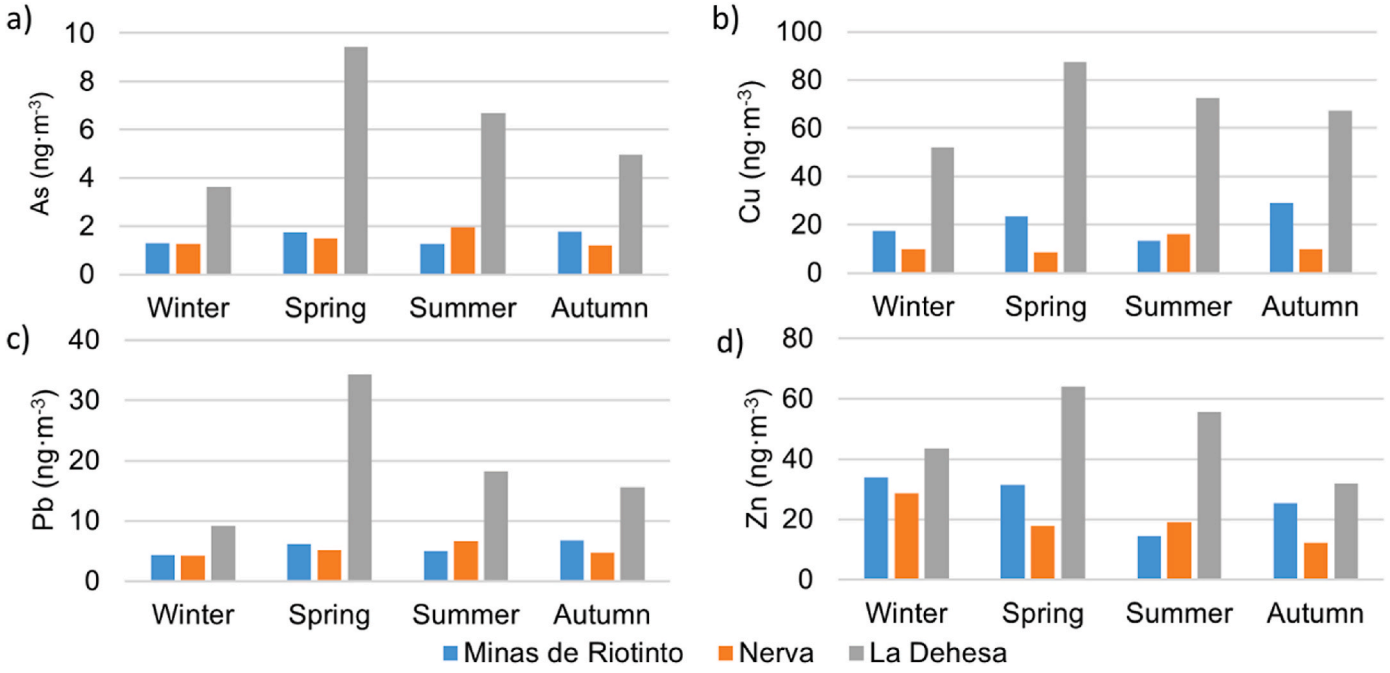

Fig. 4. Seasonal average concentrations for: a) As; b) Cu; c) Pb; and d) Zn in the three monitoring stations.

whose origin can be addressed through the source contribution analysis. Second, the village of La Dehesa (0.2 km from the mine) showed the highest concentrations of PM and PTEs, especially in the warmest seasons, thus being more potentially hazardous for human health from both physical and chemical perspectives.

3.2. Source contribution analysis

Source apportionment analysis is important to understand the degree of influence of mining operations and other sources of PM on the total pollution in populations, for this study, especially in La Dehesa, which is the most concerning result of the previous section. The source

contribution is greatly defined by the location of the monitoring stations and chemical composition of the PM samples (Hopke, 2012).

In this study, PMF analysis revealed five principal sources of PM_{10}. Two of these can be considered natural (crustal and sea salt), and three have an anthropogenic origin (regional and traffic, combustion, and mining). In La Dehesa, a second mining source, namely, Mine-2, was also observed. The chemical profiles of PM_{10} sources for Minas de Riotinto, Nerva, and La Dehesa are presented in the Supplementary Materials (Figs. SM5, SM6, and SM7, respectively).

Natural sources appeared at all three monitoring stations. The crustal source showed silicate components such as Al, Fe, Ca, and K. These are typical elements that were previously found in background soils from the Rio Tinto mining district and are derived from local dust resuspension (Vázquez-Arias et al., 2022) and Saharan outbreak dust (Rodriguez et al., 2001). An aged sea salt source was also detected with the features of marine elements Na, Cl, and Mg, as well as sulphates and nitrates. This was also previously identified on the coast of Huelva (Millán-Martínez et al., 2021), approximately 80 km to the south, revealing that seawater intrusions reach these latitudes. With respect to anthropogenic sources, the regional and traffic sources are characterised in the three stations by the presence of organic carbon and typical PTEs from vehicle exhaust emissions, such as Pb, Sb, Sn, and Bi. Moreover, Amato et al. (2014) found that these elements were also linked to non-exhaust vehicle emissions, such as road dust resuspension and tyre wear. The combustion source was dominated by elemental and organic carbons (EC and OC), NH_4, and K, which are typical elements from combustion.

The fifth source is mining, which deserves special consideration as it presents clear differences between monitoring stations. A source in Minas de Riotinto and Nerva, named Mine-1, is characterised by typical sulphide-like elements exploited from the mine: Cu, Sb, Zn, Pb, Bi, or Fe, and typical elements from the Iberian Pyrite Belt along with EC, which reveals the partial exhaust contribution. In contrast, PMF revealed an additional source of mining in La Dehesa, namely Mine-2, whose predominant elements are As, Cu, Cr, Zn, Bi, Sn, sulphates, and nitrates. To highlight the agglomeration of PTEs in the absence of K, Mg, and Fe, we assumed another pollutant source. In particular, the presence of secondary ion compounds (SICs) in this source suggests that these elements are associated with mineral extraction and processing.

The contributions of each of the previously identified sources to the monitoring stations are shown in Fig. 5. The proportion of the sea salt component is similar in the three areas (around 16–17% with annual mean concentrations ranging from 4.3 to 6.0 $\mu g/m^3$). This pattern is repeated for the crustal source (16–23%, with annual means of 5.2–7.9 $\mu g/m^3$) and combustion source (8–12%, annual mean of 2.4–4.5 $\mu g/m^3$). Major differences are found in the regional and traffic factor, which is significantly higher in Minas de Riotinto (total contribution of 43% with an annual mean of 11.2 $\mu g/m^3$) and Nerva (a contribution of 37% with annual mean 10.7 $\mu g \cdot m^{-3}$) than in La Dehesa (only 20% with an annual mean 7.5 $\mu g/m^3$). This is because Minas de Riotinto and Nerva are significantly more populated by one order of magnitude and subsequently have more traffic, which has also been observed in other studies (Boente et al., 2022; Sánchez de la Campa et al., 2020).

Notably, in La Dehesa, which is up to 0.2 km from the mine, the sum of the factors Mine-1 + Mine-2 reached 36% of the total contribution. The proximity of the monitoring station to La Dehesa may explain this division between the two mining sources, with notable contributions. However, in Nerva and Minas de Riotinto, the more distant villages from the mine, contributions are reduced to 17% (half of La Dehesa) and 8% (a fourth of La Dehesa), respectively. This results in total contributions of 13.4, 5.1, and 2.0 $\mu gPM_{10}/m^3$ in La Dehesa, Nerva, and Minas de Riotinto, respectively. The concentration found in Minas de Riotinto can be considered as the geochemical background of the area because it coincides with the levels that the mine reached during its abandonment phase (2001–2015) (Sánchez de la Campa et al., 2011). Notably, the factor Mine-2, which is practically formed by PTEs As, Cu, and Zn, has a

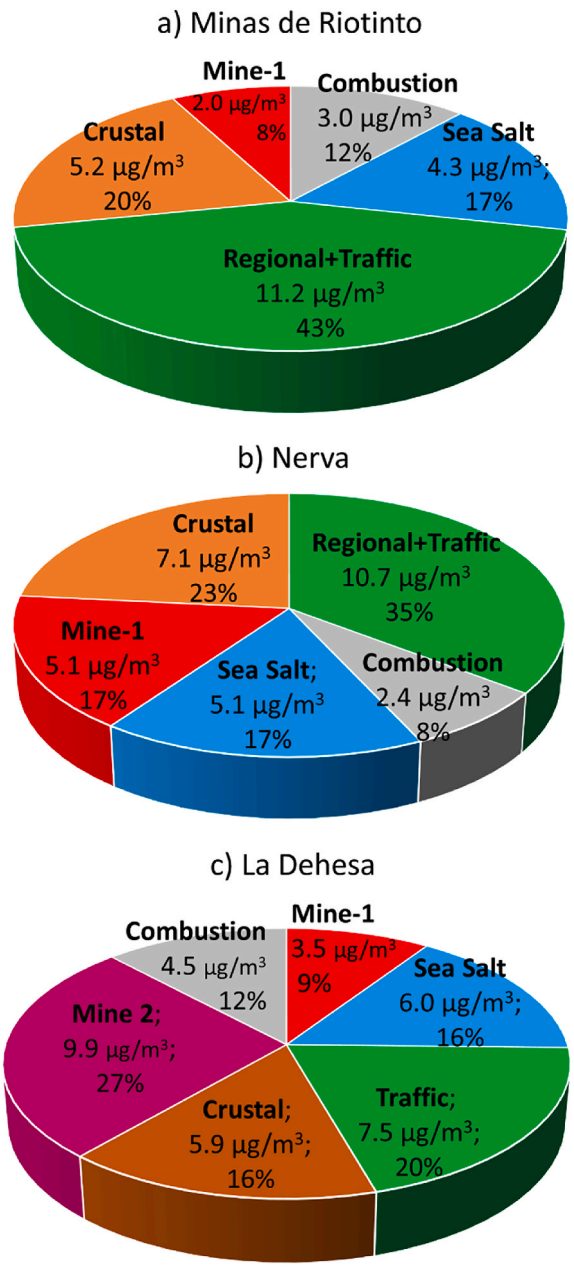

Fig. 5. Pie charts of the average source contribution (%) and mean concentration ($\mu g/m^3$) for the three monitoring stations.

contribution of 27% with the highest annual mean concentration of the monitoring station (9.9 $\mu g/m^3$). Therefore, this is a potential risk for the inhabitants of the mining village, which should be addressed through health risk assessments.

3.3. Health risk assessment

The results of the site-specific health risk assessment for the exposure scenario enabled the quantitative estimation of the probability of occurrence of any deleterious health effects in the exposed population through the inhalation of PM_{10}-bound trace elements. The hazard quotients of the potentially toxic trace elements ranged from negligible values to 0.52 for As at La Dehesa station (Table 2). Accordingly, the threshold value of 1.0 was not exceeded for any trace element of concern. The hazard index also fell within the acceptable risk level, indicating that no detrimental effects were expected from inhalation exposure to PM_{10}. However, the obtained results suggest that the

Table 2
Human health risk assessment of PM10 for non-carcinogenic elements in the monitoring stations.

SAMPLING LOCALITY			MINAS DE RIOTINTO			NERVA			LA DEHESA		
Non-carcinogenic Element	RfC[a] (mg/m^3)	Source data	C_{air} 95% UCL (mg/m^3)	EC_{inh}[b](mg/m^3)	HQ[c] (unitless)	C_{air} 95% UCL (mg/m^3)	EC_{inh}[b](mg/m^3)	HQ[c] (unitless)	C_{air} 95% UCL (mg/m^3)	EC_{inh}[b](mg/m^3)	HQ[c] (unitless)
As	1.50E-05	Cal EPA	1.89E-06	1.81E-06	0.12	1.71E-06	1.64E-06	0.11	8.06E-06	7.73E-06	0.52
Be	2.00E-05	IRIS	6.00E-08	5.75E-08	0.00	6.02E-08	5.77E-08	0.00	6.00E-08	5.75E-08	0.00
Cd	1.00E-05	ATSDR	1.00E-07	9.59E-08	0.01	1.25E-07	1.20E-07	0.01	2.00E-07	1.92E-07	0.02
Co	1.00E-04	ATSDR	3.00E-07	2.88E-07	0.00	3.54E-07	3.40E-07	0.00	1.38E-06	1.32E-06	0.01
Cu	1.00E-03	RIVM	4.10E-05	3.93E-05	0.04	1.66E-05	1.59E-05	0.02	9.14E-05	8.77E-05	0.09
Mo	4.00E-04	ATSDR	3.30E-07	3.16E-07	0.00	4.06E-07	3.89E-07	0.00	1.51E-07	1.45E-07	0.00
Ni	9.00E-05	ATSDR	4.90E-06	4.70E-06	0.05	3.66E-06	3.51E-06	0.04	6.27E-06	6.02E-06	0.07
Pb	1.50E-04	OAQPS	7.04E-06	6.75E-06	0.05	6.09E-06	5.84E-06	0.04	2.23E-05	2.14E-05	0.14
Sb	2.00E-04	IRIS	9.70E-07	9.30E-07	0.00	5.83E-07	5.59E-07	0.00	3.76E-06	3.61E-06	0.02
Se	2.00E-02	Cal EPA	1.10E-07	1.05E-07	0.00	1.35E-07	1.29E-07	0.00	1.97E-07	1.89E-07	0.00
Sn	2.10E+00	R-to-R	1.39E-06	1.33E-06	0.00	1.26E-06	1.21E-06	0.00	1.99E-06	1.91E-06	0.00
Tl	3.50E-05	R-to-R	5.00E-08	4.80E-08	0.00	5.20E-08	4.98E-08	0.00	1.13E-07	1.09E-07	0.00
V	1.00E-04	ATSDR	2.06E-06	1.98E-06	0.02	2.31E-06	2.22E-06	0.02	2.79E-06	2.67E-06	0.03
Zn	1.05E+00	R-to-R	4.36E-05	4.18E-05	0.00	4.17E-05	4.00E-05	0.00	8.08E-05	7.75E-05	0.00
Hazard Index $\sum HQ_i$					0.30	Hazard Index $\sum HQ_i$		0.25	Hazard Index $\sum HQ_i$		0.90

[a] Chemical toxicity databases: IRIS (Integrated Risk Information System), CalEPA (California Environmental Protection Agency), ATSDR (Agency for Toxic Substances and Disease Registry), RIVM (Dutch National Institute for Public Health and the Environment), OAQPS (EPA Office of Air Quality Planning and Standards), R-to-R (Route-to-Route extrapolation).
[b] As derived from the Equation: $EC_{inh} = C_{air} \times ET \times EF \times ED/AT$. For abbreviations and values used in the formula see section 2.4.
[c] As derived from the Equation: HQ $= EC_{inh}/RfC$. For abbreviations see section 2.4.

concentration and chemical composition of dust particles in La Dehesa must be monitored. The cumulative hazard index obtained at this location (HI = 0.90) was close to the regulatory limit, wherein As was the largest single contributor to the overall non-carcinogenic risk.

For carcinogen exposure (Table 3), the threshold level considered in the assessment was 1.0E-05, which is regarded in the Spanish regulatory framework (Royal Decree 9/2005 of 14th January) as the risk level of exposure that would result in no more than one excess case of cancer in 100,000 individuals exposed over a lifetime. Be, Cd, and Ni showed non-concerning risks during the entire study, with a maximum of 2.77E-07 for Ni, which is two orders of magnitude below the acceptable limit. Considering As, the estimated lifetime cancer risk values associated with inhalation exposure of all other PTEs recognised as carcinogenic or likely to be carcinogenic to humans ranged from 1.35E-06 to 2.97E-06 and 5.43E-07 to 1.19E-06 for adults and children, respectively. Therefore, although the values were close to the permissible exposure limit for carcinogens, they did not exceed the limits. However, in this case, the difference was less than one order of magnitude. Therefore, it is of vital importance to control the emissions of PM_{10} emitted by the mine to avoid reaching or surpassing the maximum limits in the future, especially after stating the notable contribution of the mine.

4. Conclusion

This study describes the impact of large metallic mines on air quality in populated areas. The research was conducted in three mining villages surrounding the Rio Tinto mine, where 248 PM_{10} filters were collected and analysed during a full year. The proposed methodology followed three steps: 1) assessing and discussing the amount of PM_{10} arriving in the mining villages; 2) conducting a source contribution analysis to discern the total contribution of the mine to PM_{10} and its chemical profiles; and 3) conducting a health risk assessment for humans to know whether the mine has adverse effects on the residents' health.

The results revealed that around a large copper mine, such as Rio Tinto, the annual and daily limit values for PM_{10} are surpassed during warm seasons, especially in villages at a close proximity to the mine. However, the degree of effect was much lower in populations further away. Additionally, we concluded that PM_{10} is highly enriched in the four PTEs that are attributable to mineralisation: As, Cu, Pb, and Zn. Following this tendency, the source contribution analysis revealed at least one mining source with a minimum contribution of 8% (2 μgPM_{10}/

Table 3
Human health risk assessment of PM10 for carcinogenic elements in the monitoring stations.

Station locality	Carcinogenic element	Element concentration 95% UCL (mg/m^3)	Inhalation Exposure Concentration (adults)[a] ECinh (mg/m^3)	Inhalation Exposure Concentration (children)[a] ECinh (mg/m^3)	Inhalation Unit Risk Factor[b] URF (μg/m^3)$^{-1}$	Cancer Risk (adults)	Cancer Risk (children)
Minas de Riotinto	As	1.89E-06	3.48E-07	1.39E-07	4.30E-03	1.50E-06	6.00E-07
	Ni	4.90E-06	9.02E-07	3.62E-07	2.40E-04	2.16E-07	8.68E-08
	Be	6.00E-08	1.10E-08	4.43E-09	2.40E-03	2.65E-08	1.06E-08
	Cd	1.00E-07	1.84E-08	7.38E-09	1.80E-03	3.31E-08	1.33E-08
Nerva	As	1.71E-06	3.15E-07	1.26E-07	4.30E-03	1.35E-06	5.43E-07
	Ni	3.66E-06	6.73E-07	2.70E-07	2.40E-04	1.62E-07	6.48E-08
	Be	6.00E-08	1.10E-08	4.43E-09	2.40E-03	2.65E-08	1.06E-08
	Cd	1.30E-07	2.39E-08	9.59E-09	1.80E-03	4.31E-08	1.73E-08
La Dehesa	As	3.76E-06	6.92E-07	2.77E-07	4.30E-03	2.97E-06	1.19E-06
	Ni	6.27E-06	1.15E-06	4.63E-07	2.40E-04	2.77E-07	1.11E-07
	Be	6.00E-08	1.10E-08	4.43E-09	2.40E-03	2.65E-08	1.06E-08
	Cd	2.00E-07	3.68E-08	1.48E-08	1.80E-03	6.62E-08	2.66E-08

[a] As derived from the Equation: $EC_{inh} = C_{air} \times ET \times EF \times ED/AT$. For abbreviations and values used in the formula see text.
[b] As specified in the USEPA's Integrated Risk Information System (IRIS).

m^3) to the total contribution in the furthest villages, but a notable 36% (13.4 $\mu gPM_{10}/m^3$) with two mining sources in the closest village: the first one was related to the mine waste, and the second one was related to the ore and presented carcinogenic PTEs. In summary, the site-specific assessment of inhalation exposure to PM_{10}-bound trace elements in the three study areas around the mining area of Rio Tinto revealed no appreciable risk of adverse non-cancer health effects attributable to the mine with the current levels of contribution. However, the risk values for As are close to the threshold values; therefore, a slight increase in mining production could lead to unacceptable levels of As.

The outcomes of this assessment have double utility because the results and methodology are easy to extrapolate to other similar cases. Moreover, the information provided here would assist mining companies in making informed decisions about the impact of mining operations on the ambient air quality and health of nearby residents.

Credit author statement

Carlos Boente: Writing – Original draft; Investigation; Data curation; Formal analysis; Software; Visualization. **Adrián Zafra-Pérez**: Writing – Original draft; Investigation; Data curation; Methodology; Software. **Juan Carlos Fernandez-Caliani:** Writing - Review and Editing; Methodology; Investigation; Supervision. **Ana Sánchez de la Campa**: Writing - Review & Editing**;** Investigation; Supervision. **Daniel Sánchez-Rodas:** Writing - Review and Editing; Resources; Investigation; Supervision **Jesús D. de la Rosa**: Writing - Review and Editing; Resources; Investigation; Conceptualization; Methodology; Supervision; Funding acquisition; Project administration.

Declaration of competing interest

The authors declare that they have no known competing financial interests or personal relationships that could have appeared to influence the work reported in this paper.

Data availability

The authors do not have permission to share data.

Acknowledgements

Carlos Boente obtained a post-doctoral contract within the program PAIDI 2020 (Ref 707 DOC 01097), the PY18-2332 Project, co-financed by the Junta de Andalucía (Andalusian Government), and Project PID2021-126986OB-I00 (Ministry of Science, Innovation and Universities of Spain), and the EU. Funding for open access charge: Universidad de Huelva / CBUA

Appendix A. Supplementary data

Supplementary data to this article can be found online at https://doi.org/10.1016/j.atmosenv.2023.119696.

References

Adame, J.A., Notario, A., Cuevas, C.A., Saiz-Lopez, A., 2022. Saharan air outflow variability in the 1980–2020 period. Sci. Total Environ. 839, 156268 https://doi.org/10.1016/j.scitotenv.2022.156268.

Amato, F., Alastuey, A., de la Rosa, J., Gonzalez Castanedo, Y., Sánchez de la Campa, A. M., Pandolfi, M., Lozano, A., Contreras González, J., Querol, X., 2014. Trends of road dust emissions contributions on ambient air particulate levels at rural, urban and industrial sites in southern Spain. Atmos. Chem. Phys. 14, 3533–3544. https://doi.org/10.5194/acp-14-3533-2014.

Amato, F., Pandolfi, M., Escrig, A., Querol, X., Alastuey, A., Pey, J., Perez, N., Hopke, P. K., 2009. Quantifying road dust resuspension in urban environment by Multilinear Engine: a comparison with PMF2. Atmos. Environ. 43, 2770–2780. https://doi.org/10.1016/j.atmosenv.2009.02.039.

Atalaya Mining, 2022. Consolidated and Company Financial Assessments, p. 2. https://atalayamining.com/wp-content/uploads/2022/03/ATYM_RNS-2021-Annual-Results-vFINAL-with-financials-1.pdf, 12.February0.2022.

Belis, C., Takahama, S., Manousakas, M.-I., Vratolis, S., Salvador, P., Decesari, S., Mircea, M., Paglione, M., Gilardoni, S., Mooibroek, D., Mocnik, G., Favez, O., Paatero, P., Diapouli, E., Vecchi, R., 2019. European Guide on Air Pollution Source Apportionment with Receptor Models. - Publications Office of the EU [WWW Document]. Jt. Res. Cent. (European Comm. URL. https://op.europa.eu/en/publication-detail/-/publication/b83f25e6-b273-11e9-9d01-01aa75ed71a1/language-en (accessed 12.20.2022).

Blais, J.F., Djedidi, Z., Cheikh, R.B., Tyagi, R.D., Mercier, G., 2008. Metals precipitation from effluents: review. Pract. Period. Hazard. Toxic, Radioact. Waste Manag. 12, 135–149. 10.1061/(ASCE)1090-025X(2008)12:3(135).

Boente, C., Gerassis, S., Albuquerque, M.T.D., Taboada, J., Gallego, J.R., 2020. Local versus regional soil screening levels to identify potentially polluted areas. Math. Geosci. 52, 381–396. https://doi.org/10.1007/s11004-019-09792-x.

Boente, C., Millán-Martínez, M., Sánchez de la Campa, A.M., Sánchez-Rodas, D., de la Rosa, J.D., 2022. Physicochemical assessment of atmospheric particulate matter emissions during open-pit mining operations in a massive sulphide ore exploitation. Atmos. Pollut. Res. 13, 101391 https://doi.org/10.1016/j.apr.2022.101391.

Brook, R.D., Rajagopalan, S., Pope, C.A., Brook, J.R., Bhatnagar, A., Diez-Roux, A.V., Holguin, F., Hong, Y., Luepker, R.V., Mittleman, M.A., Peters, A., Siscovick, D., Smith, S.C., Whitsel, L., Kaufman, J.D., 2010. Particulate matter air pollution and cardiovascular disease. Circulation 121, 2331–2378. https://doi.org/10.1161/CIR.0b013e3181dbece1.

Cabello, M., Orza, J.A.G., Dueñas, C., Liger, E., Gordo, E., Cañete, S., 2016. Back-trajectory analysis of African dust outbreaks at a coastal city in southern Spain: selection of starting heights and assessment of African and concurrent Mediterranean contributions. Atmos. Environ. 140, 10–21. https://doi.org/10.1016/j.atmosenv.2016.05.047.

Caggiano, R., Sabia, S., Speranza, A., 2019. Trace elements and human health risks assessment of finer aerosol atmospheric particles (PM1). Environ. Sci. Pollut. Res. 26, 36423–36433. https://doi.org/10.1007/s11356-019-06756-w.

Cakmak, S., Dales, R., Kauri, L.M., Mahmud, M., Van Ryswyk, K., Vanos, J., Liu, L., Kumarathasan, P., Thomson, E., Vincent, R., Weichenthal, S., 2014. Metal composition of fine particulate air pollution and acute changes in cardiorespiratory physiology. Environ. Pollut. 189, 208–214. https://doi.org/10.1016/j.envpol.2014.03.004.

Can-Terzi, B., Ficici, M., Tecer, L.H., Sofuoglu, S.C., 2021. Fine and coarse particulate matter, trace element content, and associated health risks considering respiratory deposition for Ergene Basin. Thrace. Sci. Total Environ. 754, 142026 https://doi.org/10.1016/j.scitotenv.2020.142026.

Cavalli, F., Viana, M., Yttri, K.E., Genberg, J., Putaud, J.-P., 2010. Toward a standardised thermal-optical protocol for measuring atmospheric organic and elemental carbon: the EUSAAR protocol. Atmos. Meas. Tech. 3, 79–89. https://doi.org/10.5194/amt-3-79-2010.

Cheng, X., Huang, Y., Wang, R., Ni, S.J., Long, Z.J., Liu, C., 2017. Characteristics and health risk assessment of trace metal(loid)s in PM10 at a mining city in Southwest China. Int. J. Environ. Pollut. 61, 119. https://doi.org/10.1504/IJEP.2017.085652.

Chopin, E.I.B., Alloway, B.J., 2007. Trace element partitioning and soil particle characterisation around mining and smelting areas at Tharsis, Ríotinto and Huelva, SW Spain. Sci. Total Environ. 373, 488–500. https://doi.org/10.1016/j.scitotenv.2006.11.037.

Conca, E., Abollino, O., Giacomino, A., Buoso, S., Traversi, R., Becagli, S., Grotti, M., Malandrino, M., 2019. Source identification and temporal evolution of trace elements in PM10 collected near to Ny-Ålesund (Norwegian Arctic). Atmos. Environ. 203, 153–165. https://doi.org/10.1016/j.atmosenv.2019.02.001.

Connor, J.A., Bowers, R.L., McHugh, T.H., Spexet, A.H., 2007. RBCA Tool Kit for Chemical Releases. Software Guidance Manual.

Csavina, J., Field, J., Taylor, M.P., Gao, S., Landázuri, A., Betterton, E.A., Sáez, A.E., 2012. A review on the importance of metals and metalloids in atmospheric dust and aerosol from mining operations. Sci. Total Environ. 433, 58–73. https://doi.org/10.1016/j.scitotenv.2012.06.013.

da Silva-Rêgo, L.L., de Almeida, L.A., Gasparotto, J., 2022. Toxicological effects of mining hazard elements. Energy Geosci 3, 255–262. https://doi.org/10.1016/j.engeos.2022.03.003.

De Mello, C.B., Tornos, F., Conde, C., Tassinari, C.C.G., Farci, A., Vega, R., 2022. Geology, geochemistry, and geochronology of the giant Rio tinto VMS deposit, Iberian pyrite Belt, Spain. Econ. Geol. 117, 1149–1171.

Directive 2008/50/CE, 2008. Directiva 2008/50/CE del Parlamento Europeo y del Consejo, de 21 de mayo de 2008, relativa a la calidad del aire ambiente y a una atmósfera más limpia en Europa.

Ermolin, M.S., Fedotov, P.S., Malik, N.A., Karandashev, V.K., 2018. Nanoparticles of volcanic ash as a carrier for toxic elements on the global scale. Chemosphere 200, 16–22. https://doi.org/10.1016/j.chemosphere.2018.02.089.

Fernández-Caliani, J.C., de la Rosa, J.D., Sánchez de la Campa, A.M., González-Castanedo, Y., Castillo, S., 2013. Mineralogy of atmospheric dust impacting the Rio Tinto mining area (Spain) during episodes of high metal deposition. Mineral. Mag. 77, 2793–2810. https://doi.org/10.1180/minmag.2013.077.6.07.

Fernández-Caliani, J.C., Giráldez, M.I., Barba-Brioso, C., 2019. Oral bioaccessibility and human health risk assessment of trace elements in agricultural soils impacted by acid mine drainage. Chemosphere 237, 124441. https://doi.org/10.1016/j.chemosphere.2019.124441.

Gabari, V., Fernández-Caliani, J.C., 2017. Assessment of trace element pollution and human health risks associated with cultivation of mine soil: a case study in the

Iberian Pyrite Belt. Hum. Ecol. Risk Assess. 23, 2069–2086. https://doi.org/10.1080/10807039.2017.1364130.
Gilbert, R.O., 1987. Statistical Methods for Environmental Pollution Monitoring. Van Nostrand Reinhold, New York.
Hopke, P.K., 2012. Chemical mass balance. In: Encyclopedia of Environmetrics. Wiley. https://doi.org/10.1002/9780470057339.vac017.pub2.
Huertas, J.I., Huertas, M.E., Solís, D.A., 2012. Characterization of airborne particles in an open pit mining region. Sci. Total Environ. 423, 39–46. https://doi.org/10.1016/j.scitotenv.2012.01.065.
Iarc, I.A. for R. on C., 2014. Agents Classified by the IARC Monographs, pp. 1–109.
Kabata-Pendias, A., 2010. Trace Elements in Soils and Plants. CRC Press. https://doi.org/10.1201/b10158.
Li, H., Qian, X., Wang, Q., 2013. Heavy metals in atmospheric particulate matter: a comprehensive understanding is needed for monitoring and risk mitigation. Environ. Sci. Technol. 47, 13210–13211. https://doi.org/10.1021/es404751a.
Massimi, L., Pietrantonio, E., Astolfi, M.L., Canepari, S., 2022. Innovative experimental approach for spatial mapping of source-specific risk contributions of potentially toxic trace elements in PM10. Chemosphere 307, 135871. https://doi.org/10.1016/j.chemosphere.2022.135871.
Mclaughlin, R.J.W., 1954. Iron and titanium oxides in soil clays and silts. Geochem. Cosmochim. Acta 5, 85–96. https://doi.org/10.1016/0016-7037(54)90043-5.
Men, C., Liu, R., Xu, F., Wang, Q., Guo, L., Shen, Z., 2018. Pollution characteristics, risk assessment, and source apportionment of heavy metals in road dust in Beijing, China. Sci. Total Environ. 612, 138–147. https://doi.org/10.1016/j.scitotenv.2017.08.123.
Men, C., Liu, R., Xu, L., Wang, Q., Guo, L., Miao, Y., Shen, Z., 2020. Source-specific ecological risk analysis and critical source identification of heavy metals in road dust in Beijing, China. J. Hazard Mater. 388, 121763 https://doi.org/10.1016/j.jhazmat.2019.121763.
Millán-Martínez, M., Sánchez-Rodas, D., Sánchez de la Campa, A.M., de la Rosa, J., 2021. Contribution of anthropogenic and natural sources in PM10 during North African dust events in Southern Europe. Environ. Pollut. 290, 118065 https://doi.org/10.1016/j.envpol.2021.118065.
Moreno, T., Trechera, P., Querol, X., Lah, R., Johnson, D., Wrana, A., Williamson, B., 2019. Trace element fractionation between PM10 and PM2.5 in coal mine dust: Implications for occupational respiratory health. Int. J. Coal Geol. 203, 52–59. https://doi.org/10.1016/j.coal.2019.01.006.
Müller, M., 2022. Meteoblue: weather close to you. https://www.meteoblue.com/ (accessed 12.February.2022).
Naraki, H., Keshavarzi, B., Zarei, M., Moore, F., Abbasi, S., Kelly, F.J., Dominguez, A.O., Jaafarzadeh, N., 2021. Urban street dust in the Middle East oldest oil refinery zone: oxidative potential, source apportionment‹ and health risk assessment of potentially toxic elements. Chemosphere 268, 128825. https://doi.org/10.1016/j.chemosphere.2020.128825.
Nie, D., Wu, Y., Chen, M., Liu, H., Zhang, K., Ge, P., Yuan, Y., Ge, X., 2018. Bioaccessibility and health risk of trace elements in fine particulate matter in different simulated body fluids. Atmos. Environ. 186, 1–8. https://doi.org/10.1016/j.atmosenv.2018.05.024.
Norris, G., Duvall, R., 2014. EPA Positive Matrix Factorization (PMF) 5.0 Fundamentals and User Guide. EPA 600/R-08/108.
Paatero, P., 1997. Least squares formulation of robust non-negative factor analysis. Chemometr. Intell. Lab. Syst. 37, 23–35. https://doi.org/10.1016/S0169-7439(96)00044-5.
Paatero, P., Hopke, P.K., 2003. Discarding or downweighting high-noise variables in factor analytic models. Anal. Chim. Acta 490, 277–289. https://doi.org/10.1016/S0003-2670(02)01643-4.
Paatero, P., Tapper, U., 1994. Positive matrix factorization: a non-negative factor model with optimal utilization of error estimates of data values. Environmetrics 5, 111–126. https://doi.org/10.1002/env.3170050203.
Pandey, B., Agrawal, M., Singh, S., 2014. Assessment of air pollution around coal mining area: emphasizing on spatial distributions, seasonal variations and heavy metals, using cluster and principal component analysis. Atmos. Pollut. Res. 5, 79–86. https://doi.org/10.5094/APR.2014.010.
Parviainen, A., Vázquez-Arias, A., Arrebola, J.P., Martín-Peinado, F.J., 2022. Human health risks associated with urban soils in mining areas. Environ. Res. 206, 112514 https://doi.org/10.1016/j.envres.2021.112514.
Patra, A.K., Gautam, S., Kumar, P., 2016. Emissions and human health impact of particulate matter from surface mining operation—a review. Environ. Technol. Innov. 5, 233–249. https://doi.org/10.1016/j.eti.2016.04.002.
Peled, R., 2011. Air pollution exposure: who is at high risk? Atmos. Environ. 45, 1781–1785. https://doi.org/10.1016/j.atmosenv.2011.01.001.
Pless-Mulloli, T., 2000. Living near opencast coal mining sites and children's respiratory health. Occup. Environ. Med. 57, 145–151. https://doi.org/10.1136/oem.57.3.145.
Querol, X., Alastuey, A., Rosa, J. de la, Sánchez-de-la-Campa, A., Plana, F., Ruiz, C.R., 2002. Source apportionment analysis of atmospheric particulates in an industrialised urban site in southwestern Spain. Atmos. Environ. 36, 3113–3125. https://doi.org/10.1016/S1352-2310(02)00257-1.
Ramírez, O., Sánchez de la Campa, A.M., Sánchez-Rodas, D., de la Rosa, J.D., 2020. Hazardous trace elements in thoracic fraction of airborne particulate matter: assessment of temporal variations, sources, and health risks in a megacity. Sci. Total Environ. 710, 136344 https://doi.org/10.1016/j.scitotenv.2019.136344.
Rodriguez, S., Querol, X., Alastuey, A., Kallos, G., Kakaliagou, O., 2001. Saharan dust contributions to PM10 and TSP levels in Southern and Eastern Spain. Atmos. Environ. 35, 2433–2447. https://doi.org/10.1016/S1352-2310(00)00496-9.
Royal Decree 102/2011, 28 January, 2011. Real Decreto 102/2011, de 28 de enero, relativo a la mejora de la calidad del aire.
Royal Decree 9/2005, 14 January, 2005. Real Decreto 9/2005, de 14 de enero, por el que se establece la relación de actividades potencialmente contaminantes del suelo y los criterios y estándares para la declaración de suelos contaminados.
Ruggieri, F., Fernandez-Turiel, J.L., Saavedra, J., Gimeno, D., Polanco, E., Amigo, A., Galindo, G., Caselli, A., 2012. Contribution of volcanic ashes to the regional geochemical balance: the 2008 eruption of Chaitén volcano, Southern Chile. Sci. Total Environ. 425, 75–88. https://doi.org/10.1016/j.scitotenv.2012.03.011.
Sáez, R., Almodóvar, G.R., Pascual, E., 1996. Geological constraints on massive sulphide genesis in the Iberian Pyrite Belt. Ore Geol. Rev. 11, 429–451. https://doi.org/10.1016/S0169-1368(96)00012-1.
Salkield, L.U., 1987. A Technical History of the Rio Tinto Mines: Some Notes on Exploitation from Pre-Phoenician Times to the 1950s. The Institution of Mining and Metallurgy, London, p. 116.
Sánchez de la Campa, A.M., Sánchez-Rodas, D., Márquez, G., Romero, E., de la Rosa, J. D., 2020. 2009–2017 trends of PM10 in the legendary Riotinto mining district of SW Spain. Atmos. Res. 238, 104878 https://doi.org/10.1016/j.atmosres.2020.104878.
Sánchez de la Campa, A.M., de la Rosa, J.D., Fernández-Caliani, J.C., González-Castanedo, Y., 2011. Impact of abandoned mine waste on atmospheric respirable particulate matter in the historic mining district of Rio Tinto (Iberian Pyrite Belt). Environ. Res. 111, 1018–1023. https://doi.org/10.1016/j.envres.2011.07.001.
Sastry, V.R., Chandar, K.R., Nagesha, K.V., Muralidhar, E., Mohiuddin, M.S., 2015. Prediction and analysis of dust dispersion from drilling operation in opencast coal mines. Procedia Earth Planet. Sci. 11, 303–311. https://doi.org/10.1016/j.proeps.2015.06.065.
Stein, A.F., Draxler, R.R., Rolph, G.D., Stunder, B.J.B., Cohen, M.D., Ngan, F., 2015. NOAA's HYSPLIT atmospheric transport and dispersion modeling system. Bull. Am. Meteorol. Soc. 96, 2059–2077. https://doi.org/10.1175/BAMS-D-14-00110.1.
Stewart, A.G., 2020. Mining is bad for health: a voyage of discovery. Environ. Geochem. Health 42, 1153–1165. https://doi.org/10.1007/s10653-019-00367-7.
Tubis, A., Werbińska-Wojciechowska, S., Wroblewski, A., 2020. Risk assessment methods in mining industry—a systematic review. Appl. Sci. 10, 5172. https://doi.org/10.3390/app10155172.
Ulniković, V.P., Kurilić, S.M., 2020. Heavy metal and metalloid contamination and health risk assessment in spring water on the territory of Belgrade City, Serbia. Environ. Geochem. Health 42, 3731–3751. https://doi.org/10.1007/S10653-020-00617-Z/TABLES/4.
UNE, S.A. for S., 2015. UNE-EN 12341. Ambient Air - Standard Gravimetric Measurement Method for the 694 Determination of the PM10 or PM2,5 Mass Concentration of Suspended Particulate Matter. URL. https://www.une.org/encuentra-tu-norma/busca-tu-norma/norma?c=N0054246 (accessed 10.26.22).
UNE, S.A. for S., 2008. UNE-EN ISO 9001:2008. Quality Management Systems - Requirements. URL. https://www.une.org/encuentra-tu-norma/busca-tu-norma/norma/?Tipo=N&c=N0042135 (accessed 2.20.2023).
USEPA, 1986. Guidelines for Carcinogen Risk Assessment. EPA/630/R-00/004.
USEPA, 1989. Risk Assessment Guidance for Superfund, Volume I, Human Health Evaluation Manual (Part A). EPA/540/1-89/002.
USEPA, 1992. Supplemental Guidance to Risk Assessment Guidance for Superfund: Calculating the Concentration Term.
USEPA, 2009. Risk assessment guidance for superfund volume I: human health evaluation manual (Part F, supplemental guidance for inhalation risk assessment). OSWER 9285, 7–82. EPA-540-R-070-002.
Utembe, W., Faustman, E., Matatiele, P., Gulumian, M., 2015. Hazards identified and the need for health risk assessment in the South African mining industry. Hum. Exp. Toxicol. 34, 1212–1221. https://doi.org/10.1177/0960327115600370.
Van Den Heuvel, R., Den Hond, E., Govarts, E., Colles, A., Koppen, G., Staelens, J., Mampaey, M., Janssen, N., Schoeters, G., 2016. Identification of PM 10 characteristics involved in cellular responses in human bronchial epithelial cells (Beas-2B). Environ. Res. 149, 48–56. https://doi.org/10.1016/j.envres.2016.04.029.
Vardoulakis, S., Kassomenos, P., 2008. Sources and factors affecting PM10 levels in two European cities: Implications for local air quality management. Atmos. Environ. 42, 3949–3963. https://doi.org/10.1016/j.atmosenv.2006.12.021.
Vázquez-Arias, A., Martín Peinado, F., Parviainen, A., 2022. Effect of Parent Material and Atmospheric Deposition on the Potential Pollution of Urban Soils Close to Mining Areas. https://doi.org/10.22541/au.165470055.56054250/v1.
Verginelli, I., Nocentini, M., Baciocchi, R., 2017. An alternative screening model for the estimation of outdoor air concentration at large contaminated sites. Atmos. Environ. 165, 349–358. https://doi.org/10.1016/j.atmosenv.2017.06.052.
Viana, M., Querol, X., Alastuey, A., Cuevas, E., Rodriguez, S., 2002. Influence of African dust on the levels of atmospheric particulates in the Canary Islands air quality network. Atmos. Environ. 36, 5861–5875. https://doi.org/10.1016/S1352-2310(02)00463-6.
Wild, P., Bourgkard, E., Paris, C., 2009. Lung Cancer and Exposure to Metals: the Epidemiological Evidence, pp. 139–167. https://doi.org/10.1007/978-1-60327-492-0_6.
Zafra-Pérez, A., Boente, C., de la Campa, A.S., Gómez-Galán, J.A., de la Rosa, J.D., 2023. A novel application of mobile low-cost sensors for atmospheric particulate matter monitoring in open-pit mines. Environ. Technol. Innov. 29, 102974 https://doi.org/10.1016/j.eti.2022.102974.